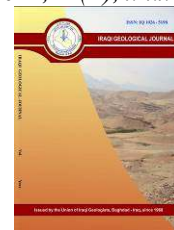




Iraqi Geological Journal

Journal homepage: <https://www.igi-iraq.org>



Structure Boundary Separating Using Gravity Data For Central And Southern Parts Of The East Java Basin Beneath The Quaternary Volcanic Deposits

Ardian Novianto^{1,2}, Sutanto¹, Suharsono², Carolus Prasetyadi¹ and Jatmiko Setiawan¹

¹ Geological Engineering UPN "Veteran" Yogyakarta, Indonesia 1; ardian.novianto@upnyk.ac.id

² Geological Engineering UPN "Veteran" Yogyakarta, Indonesia 1; sutanto@upnyk.ac.id

³ Geophysical Engineering UPN "Veteran" Yogyakarta, Indonesia 2; suharsono.geofisika@upnyk.ac.id

⁴ Geological Engineering UPN "Veteran" Yogyakarta, Indonesia 1; cprasetyadi@upnyk.ac.id

⁵ Geological Engineering UPN "Veteran" Yogyakarta, Indonesia 1; jatmikosetiawan@upnyk.ac.id

* Correspondence: ardian.novianto@upnyk.ac.id

Received: date; Accepted: date; Published: date

Abstract

Stratigraphic interpretation shows that the relationship between Cenozoic volcanic rocks deposited in the Southern Mountains and marine clastic volcanic rocks in the Kendeng Basin possibly forms a stratigraphic transition bordered by the major fault that is yet to be defined. The thick Quaternary volcanic deposits obstruct field observation on the surface. Miocene outcrops in limited presence are found on the volcanic slope, positioned relatively more to the north than the same outcrop. This feature indicates major thrusting in southern Java that moved it to the north. The gravity data analysis was used to obtain the field observation and identify the subsurface geology. Total Horizontal Derivative analysis of the gravity data showed a major fault boundary with a relative west-east direction separating the high Bouguer anomaly area in the south from a large negative area of about -50 mGal in the north. Second Vertical Derivative analysis reconstructed the fault slope direction and showed a south-facing slope with a large angle. Based on the combination of the surface data and the subsurface analysis, the boundary is a major fault with a west-east direction on the south side of the Quaternary volcanic range and a south-facing slope. It is interpreted as the result of the compressive tectonics that formed the fold-thrust belt system.

Keywords: East Java Basin; Fold-Thrust Belt System; Derivative Gravity

1. Introduction

The physiographic of East Java, Indonesia, from the north to the south can be generally divided into three parts, namely Rembang, Kendeng, and Southern Mountains Zones (Smyth et al., 2005; Smyth et al., 2008). The Kendeng Zone is separated from the Southern Mountains by an area composed of volcanoes and Quaternary volcanic deposits known as the Ngawi subzone (Setiaji et al. 2016; Van Bemmelen, 1949) (**Fig. 1**). This zone is a sedimentary basin with a relative west-east orientation and divides East Java into three basin: the northern, central, and southern basins. Meanwhile, the Rembang Zone represents a basin at the edge of the Sunda Shelf composed of shallow marine deposits. To the

35 south, there is a deep basin filled with deep-sea clastic volcanic deposits, otherwise known as the
36 Kendeng Basin. Finally, the southernmost basin consists of Eocene-Miocene volcanic deposits known
37 as the Early Cenozoic Southern Mountain Arc.

38 These basins share boundaries in the form of geological features: the Rembang and the Kendeng
39 Basins are separated by the Randublatung High identified as a faulting block extending west-east
40 (Prasetyadi et al., 2016), and the Kendeng Basin and the Southern Mountains by a young Quaternary
41 volcanic arc. The Quaternary volcanic deposits pose significant challenges in depicting subsurface
42 geology. The stratigraphic or structural feature separating the Kendeng Basin from the Southern
43 Mountains is not identifiable from the surface. Some scholars have defined the two basins based solely
44 on morphological conditions distinguishing the Southern Mountains from the Quaternary volcanic
45 deposits, implying that the precise boundaries have yet to be identified. This problem, however, can be
46 addressed by a subsurface study using the gravity method to analyze the boundary between the Kendeng
47 Basin and the Southern Mountains.

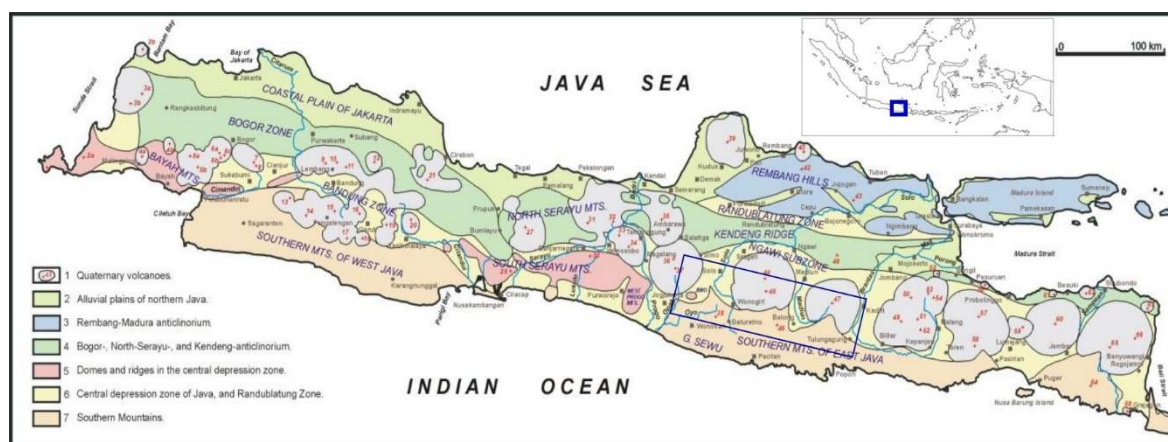
48 The Quaternary Volcanic Arc Line occupies the southern part of East Java and covers most of the
49 southern part of the Kendeng Basin. This young volcanic deposit has been active since the Late Miocene
50 (Smyth et al., 2005). It is interpreted as thick deposits, which raises a problem in the subsurface
51 interpretation of the developing stratigraphy and geological structures, especially at the interface
52 between the Kendeng Basin and the Southern Mountains. The stratigraphy of the Southern Mountains
53 can be recognized from the Eocene-Miocene outcrops developing as siliciclastic, volcanoclastic,
54 volcanic, and carbonate sediments. On the contrary, rocks of the same age constituting the Kendeng
55 Basin are covered by the Quaternary volcanic deposits and are generally not visible on the surface. The
56 interface between the two zones is interpreted as a stratigraphic transition from volcanic arc products to
57 volcanogenic and pelagic sediments. During Oligocene-Miocene, the volcanic arc products filled the
58 Kendeng Basin in the north and caused sediment loading, creating a deep flexural basin (Waltham et al.,
59 2008). Rocks in the Kendeng Basin are rarely exposed, but interpretation shows that the rock sequence
60 thickens to the south towards the Southern Mountains (Hall et al., 2007).

61 In general, rocks in the Southern Mountains are currently sloping to the south with low dip angles
62 where contact with rocks in the Kendeng Basin in the north is unexposed. As a result, the interzonal
63 boundaries are currently not identifiable. Some arguments connect the two basins with sediments that
64 change gradually and experience tectonics producing anticline remnants with an eroded limb in the
65 north. Other researchers suggest that the interzonal boundary is a faulting block formed due to
66 extensional tectonics. However, the idea of extensional tectonics as the forces generating the fault block
67 raises objections, as evidenced by satellite image analysis and microtectonics studies that conclude the
68 slopes of Baturagung, south of Bayat (Jiwo Hill), Central Java, Indonesia, as a result of a compressive
69 tectonic regime (Husein et al., 2008).

70 Various possible tectonics acting on the southern part of the East Java Basin indicate compressive
71 tectonics. This compressive tectonics concept conforms to the subduction concept because of the
72 movement of the Gondwana microcontinent in southern Java during the Cenozoic. Several experts, e.g.,
73 Hall et al., 2007, have put forward relevant indications as inferred from the well-developed compressive
74 tectonics in the Southern Mountains that generate a thrust fault uplifting the old rocks to the north.
75 Husein et al., 2008 provides the surface evidence to the rock displacement, that is, a thrust fault with an
76 imbricate fan system and a duplex structure in the Tegalorejo area, south of Bayat, Central Java. The
77 thrust fault is interpreted as being formed at the base of the northern mountain range and spanning to
78 the northern edge of the Wonosari Basin (depression), which is the northern part of the Southern
79 Mountains (Hall et al., 2007). The position of the northern boundary of this thrust fault system, which
80 marks the interface between the Kendeng Basin and the Southern Mountains, remains open to debate.
81 Because of the overlying Quaternary volcanic deposits, the concept of the thrust fault is not indicated.
82 This study sought to determine the northern boundary of the thrust fault system in a subsurface study

83 using the gravity method. The determination of fault position will have implications for the concept of
 84 hydrocarbon exploration, especially for the potential of reservoir rocks which are interpreted to form
 85 structures trap due to compression tectonic processes.

86



87

88 **Fig.1.** Schematic Physiographic Map of Java and Madura (Indonesia) divides eastern Java into several
 89 physiographic zones and shows the distribution of Quaternary volcanic deposits in the south (after Van Bemmelen,
 90 1970) (Setiaji et al., 2016). The blue-line box marks the research location.

91

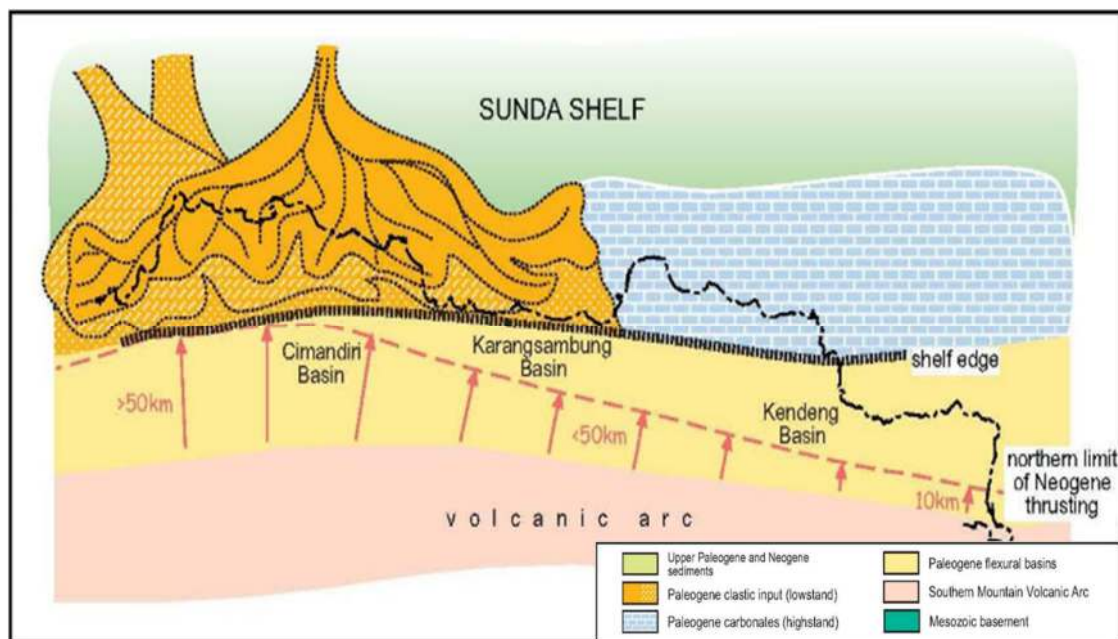
92 2. Tectonic Setting

93 The compressive tectonics at work along southern Java is a long-standing concept that continues to
 94 develop. This area, lying in a forearc tectonic setting, experienced compression forces from the
 95 subduction process occurring in several periods in the Cenozoic. Some evidence of this compressive
 96 tectonic system has been found throughout the island, especially in the east. The system generated major
 97 thrusting of varying intensity in the south and displaced Paleogene volcanic rocks to the north (Hall et
 98 al., 2007), although the intensity becomes increasingly weaker eastward (**Fig. 2**).

99 Northward thrusting in eastern Java is relatively less distinct from the one occurring on the western
 100 side. Based on stratigraphic contact, the northward thrusting is indicated by Paleogene outcrops in the
 101 Southern Mountains. On the contrary, rocks of the same age are not found in the north (part of the
 102 Kendeng Basin). Some have made assumptions about this condition: although field observations show
 103 that Quaternary volcanic deposits have developed at the interzonal boundary, the idea that the northern
 104 zone is part of the footwall of the thrust fault system remains a debatable matter. The development of
 105 the northward thrusting can even be traced to the northern margin of the Kendeng Basin that borders the
 106 Rembang Basin. The northward thrusting in this location created folds; hence, it is known as the
 107 Kendeng fold-thrust belt system.

108 The structural concept of the thrust fault system is also found in several places in the northern part
 109 of the Southern Mountain Range. Many pretertiary and Paleogene outcrops are found in Bayat, which
 110 is the western part of the Southern Mountain Range and the thrust fault system. Indications of this
 111 structure, i.e., the Old Andesite Formation (OAF) contacts that experience substantial deformation, are
 112 also found in several locations in the east.

113



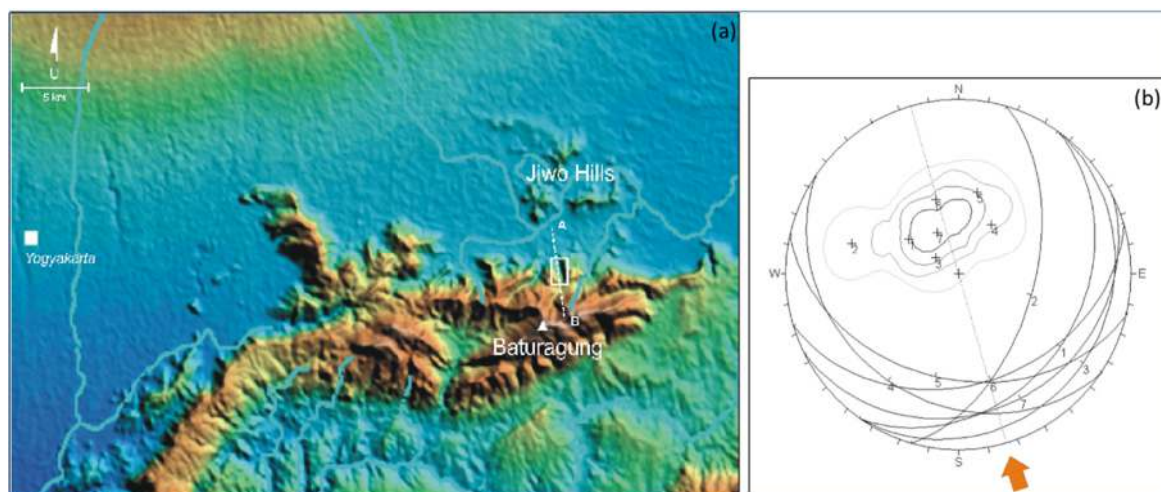
114 **Fig. 2.** Schematic image shows the northward thrusting in the south of Java that moved the Paleogene volcanic arc
 115 further north (Hall et al., 2007).
 116
 117

118 **Baturagung Mountain Range**

119 The Baturagung Mountain Range is the western part of the Southern Mountains with a high
 120 topography that forms a cuesta with southeast-facing slopes. In the north of the range, a steep slope
 121 marks the northern margin of the Southern Mountains (**Fig. 3a**). Stratigraphically, the mountain range
 122 is composed of volcanoclastic sediments from the Oligocene Kebobutak and Semilir Formations.
 123 Approximately 2 km to the north, an important stratigraphic relationship is found, viz. pretertiary
 124 basement complex in Jiwo Hills (Bayat) that appears an outcrop.

125 Many scholars have explained the concept of the Compressive Tectonic Play that forms the
 126 Baturagung Mountain Range. Compressive Tectonic Play is identified by the broad anticline structure
 127 with northward upthrust at the base of this anticline. Similarly, Van Bemmelen, 1949 interprets the
 128 Baturagung Mountain Range as a result of northward transformation from a normal fault to a wide
 129 monocline due to Listrik fault in Wonosari Basin (Husein et al., 2008).

130 Evidence of the Compressive Tectonic Play can be found in the Tegalrejo thrust fault system
 131 (Husein et al., 2008), which changes the steep physiography of the Baturagung Mountain Range into
 132 the lowlands in the north (Klaten), wherein pretertiary rock complex is visible on the surface. There are
 133 seven thrust faults at this location forming the imbricate fan and duplex structures. A previous simple
 134 stereographic analysis concludes that the thrust fault system has moved the coarse sandstone from the
 135 SSE direction or approximately N073°E (**Fig. 3b**). At a nearby location, a plunging anticline forms a
 136 fault-propagation fold system, which is steep in the north. The fold axis shows the NE-SW direction due
 137 to the compressive force coming from the NW-SE direction. The force in question has the same direction
 138 as the thrust fault system found in the Tegalrejo area; thus, it can be inferred that the same compression
 139 event is responsible for the two structures and produces the fold-thrust belt system that forms the
 140 Baturagung Mountain Range.
 141



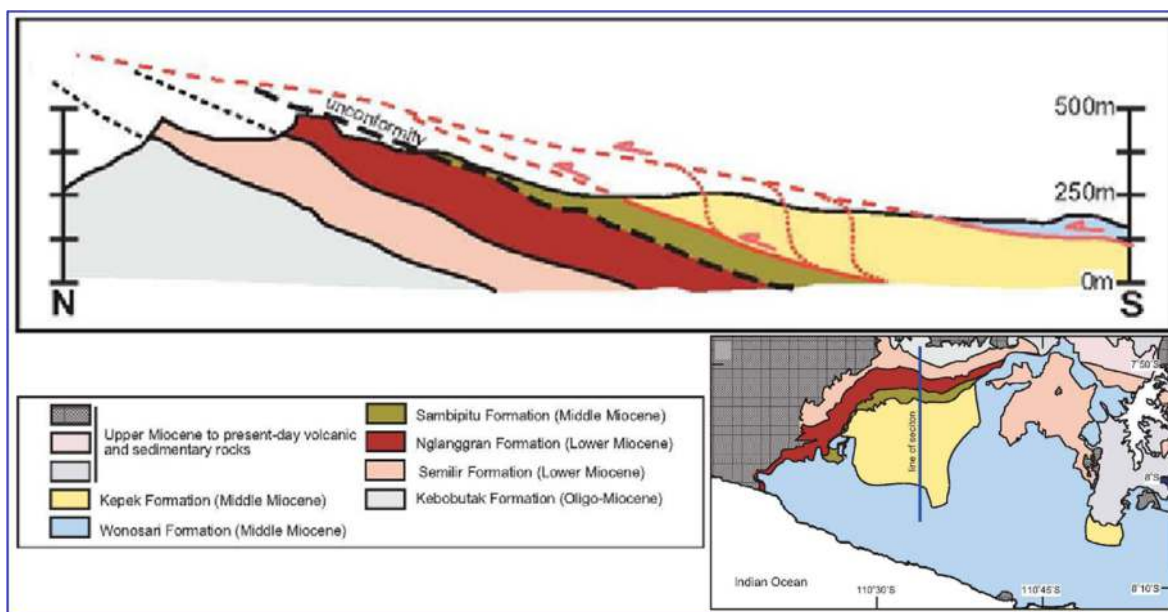
142
143 **Fig. 3.** (a) Physiography of the Baturagung Range and (b) stereograph projection show the direction of the
144 Tegalrejo-Bayat Thrust Fault System movement. The direction of the stress indicates that it originates from the
145 SSE (N073°E), perpendicular to the acting force, and proves the concept of compressional tectonics in this region
146 (Hussein et al., 2008).
147

148 **Wonosari Trough**

149 The Oligocene volcanic activity producing the constituent rocks of the Baturagung Mountain Range
150 began to weaken in the Lower-Middle Miocene (Smyth et al., 2005). This volcanic activity occurred in
151 subaerial to shallow marine environments. Simultaneously, with the end or weakening of this tectonic
152 activity, the Sambipitu, Wonosari, and Kepek Formations were deposited discontinuously (or in
153 unconformity) in the Wonosari Trough. The Wonosari Trough is interpreted as a narrow basin bordered
154 by the Baturagung Mountain Range to the north and the Carbonate Platform of the Wonosari Formation
155 to the south (Hall et al., 2007). It extends as far as 45 km with a relative east-west direction and a width
156 of approximately 5–10 km. Its northern and southern highs are thought to supply most volcanic-rich
157 sediments and carbonate fragments of Sambipitu and Kepek Formations that are deposited in the trough.

158 Sambipitu Formation is composed of rocks rich in volcanic material and contains minute amounts
159 of carbonate deposited in a turbidite system. Currently, the formation has level topography and is
160 bordered by mountains with steep reliefs that are part of the Baturagung Mountain Range north of the
161 southern mountain range. The stratigraphy of the boundary shared by the Sambipitu Formation and the
162 Baturagung Mountain Range cannot be clearly explained because of the sudden change from the
163 volcanic deposits stretching from the subaerial to shallow marine environments of the Baturagung
164 Mountain Range to the deep-sea deposits of Sambipitu Formation with a turbidite system (Hall et al.,
165 2007). On the other hand, in the south, Kepek Formation contains more carbonate material resulting
166 from the breaking down of the Wonosari Carbonate Platform. This formation is composed of turbidite
167 sequences rich in carbonate debris that gradually changes from the Wonosari Formation.

168 This geological overview shows a sudden change from shallow to deep-sea deposits, implying rapid
169 local subsidence that forms a narrow and deep basin following the end of volcanism in the Oligo-
170 Miocene. In addition, the sudden change indicates a compressive tectonic concept that generates thrust
171 faults in the southern mountain range. The northward thrust fault uplifted the southern part and formed
172 a basin in the north. As a result, the Wonosari Platform experienced northward thrust fault, covering the
173 Sambipitu Formation (**Fig. 4**) (Hall et al., 2007).
174
175
176
177
178



179
180 **Fig. 4.** Schematic cross-sections interpret the thrust fault system of the limestone of the Wonosari, Kepek, and
181 Sambipitu Formations as parts of the Wonosari Trough deposits and the underlying Lower Miocene volcanic rocks
182 (Hall et al., 2007).
183

184 Prigi Deformation

185 Prigi is located in eastern Java, notably east of the Southern Mountain Range. The stratigraphy of
186 this area begins with the deposition of volcanic rocks from the Lower Miocene Mandalika Formation
187 and is followed by the deposition of the Campurdarat Formation. The Campurdarat Formation is
188 dominated by limestone with clay inserts and is volcanoclastic (Smyth et al., 2005). Limestone contains
189 volcanoclastic debris and faunal assemblage—indicating Middle Miocene—which in some places show
190 a slumping structure. Geology interpretation defines the depositional environment of this formation as
191 shallow seas close to volcanic sources, meaning that the environment contains a mixture of volcanic
192 debris and shallow marine bioclasts. The Mandalika and Campurdarat Formations generally show a
193 small dip sloping to the south. Some places show strong deformation that generated a plunging fold with
194 a low angle towards the northwest (Hall et al., 2007). The strong deformation indicates a thrust fault at
195 the base of the Southern Mountains zone.

196 Field observations indicate the presence of compressive tectonics along the Southern Mountains.
197 Hall et al., 2007 reconstructs the process by which compressive tectonics generated major thrusting in
198 southern Java that displaced Paleogene volcanic rocks to the north (**Fig. 2**). The intensity of the major
199 thrusting becomes increasingly larger to the west, wherein the magnitude of the northward thrusting
200 ranged from 10 km in East Java to 50 km in West Java (Hall et al., 2007). The thrusting is thought to
201 occur in the Early Miocene, and the formation process possibly lasted for more than one period, which
202 coincided with the cessation of the Paleogene volcanic phase in Java—as marked by the Australia-SE
203 Asia collision in eastern Indonesia (Hall et al., 2007).

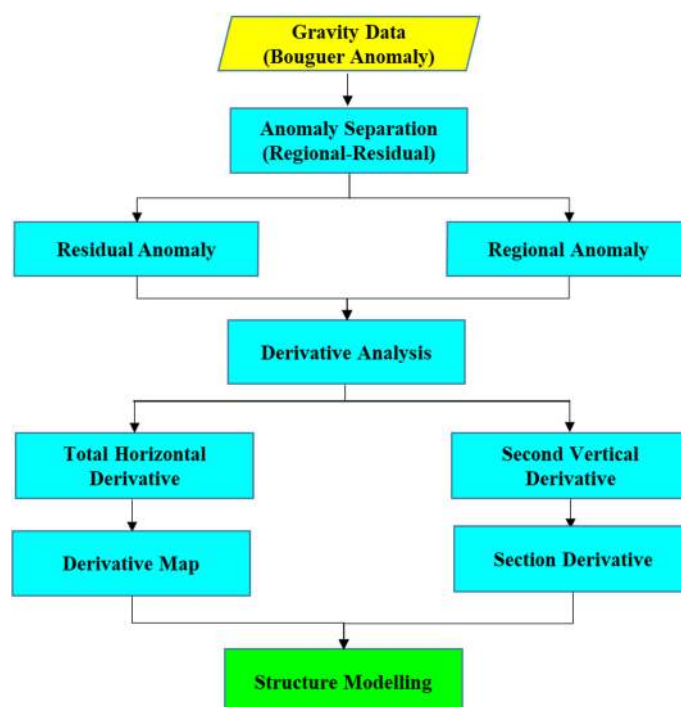
204 3. Materials and Methods

205 Several geologists have put forward the interzonal boundary between the Southern Mountains and
206 the Kendeng Basin. Van Bemmelen, 1949, physiographically defines the northern margin of the
207 Southern Mountains as a volcanic deposit zone identified as the Ngawi subzone (**Fig. 1**). The gravity
208 data show another pattern where the Southern Mountains zone is directly adjacent to the low gravity
209 anomaly area in the Kendeng Basin in the north; hence, it can be inferred that the boundary between the
210 two zones is relatively more to the south (Smyth et al., 2008).

211 The subsurface geological conditions cannot be clearly identified at this boundary as it is nearly
 212 entirely covered by Quaternary volcanic deposits. As a result, the northward distribution of Oligo-
 213 Miocene outcrops in the Southern Mountains (to the Kendeng Basin) is unknown. Similarly, the
 214 subsurface continuity of the thrust fault concept that is otherwise visible on the surface from the south
 215 to the middle of the Southern Mountains and controls the development of geological structures in the
 216 two basins cannot be precisely defined. Therefore, the position of the structural boundary separating
 217 them has not been determined due to the overlying Quaternary volcanic deposits.

218 Indications of subsurface faults, notably those separating the two basins, are revealed in this study
 219 based on the derivative analysis of the gravity data, as shown in the research flow chart in **Fig. 5**. The
 220 gravity data used is based on measurements made by the Geological Research and Development Center,
 221 Indonesia, that are presented in the Bouguer anomaly map on Surakarta, Ponorogo, and Madiun sheets.
 222 The Bouguer anomaly comprises local and regional gravity anomalies or, to simplify, shallow and deep
 223 gravity anomalies. Structures affecting the geological order in this area are interpreted as related to the
 224 basement development in the study area, meaning that the gravity data analysis needs to focus on
 225 regional anomalies. This analysis started with filtering to separate regional and residual anomalies. The
 226 derivative analysis of the regional gravity anomaly aimed to highlight the effects produced by faults.
 227 Horizontal and vertical derivative analyses are often used to increase the anomaly at the boundary of an
 228 anomaly source (Sumintadireja et al., 2018). For instance, an anomaly source may be caused by the
 229 presence of faults or the boundary of a sedimentary basin.

230



231

232

Fig. 5. Research methodology flow diagram

233 Second Vertical Derivative (SVD) is often used to enhance fine-sized features that are not visually
 234 visible in the original gravity data. The results, both gradient and magnitude, can be used to describe the
 235 boundary of the anomaly caused by the fault observed. A high gradient is associated with a large contrast
 236 of physical properties and vice versa, in subsurface conditions (Sumintadireja et al., 2018). SDV can be
 237 calculated in Fourier (wavenumber) and spatial domains. In the Fast Fourier Transform domain, the
 238 derivatives of all directions can be calculated. This process increases the high-frequency components in
 239 the gravity data, as shown in the equation below:

240

241
$$\frac{\partial^2 g_z}{\partial z^2} = F^{-1}(|k|^2 G_z) \quad \text{with} \quad |k|^2 = k_x^2 + k_y^2 \quad (1)$$

242
 243 where G_z is the Fourier transform of g_z , k_x and k_y are wavenumbers on the x and y axes,
 244 respectively, and F^{-1} is the inverse operator of the Fourier transform.

245 SVD can also be computed in the spatial domain of its horizontal gradient using the Laplace
 246 equation:

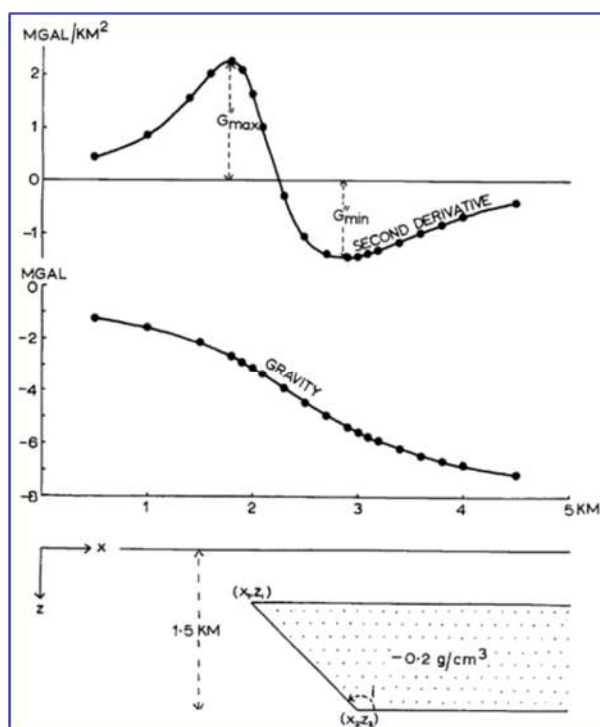
247
 248
$$\frac{\partial^2 g_z}{\partial z^2} = - \left(\frac{\partial^2 g_z}{\partial x^2} + \frac{\partial^2 g_z}{\partial y^2} \right) \quad (2)$$

249
 250 Bott, 1962, has developed simple criteria for interpreting gravity anomalies based on the SVD's
 251 relative magnitude or [g''] in the 1D gravity profile. For example, the SVD value of the gravity anomaly
 252 at the two-dimensional horizontal slab with a sloping edge at the position $(x, 0)$ can be written as:

253
 254
$$g'' = -2K\rho \sin i \left[\frac{(x_1-x) \sin i - z_1 \cos i}{(x_1-x)^2 + z_1^2} - \frac{(x_2-x) \sin i - z_2 \cos i}{(x_2-x)^2 + z_2^2} \right] \quad (3)$$

255
 256 where K is the gravitational constant, ρ is the rock's density contrast, i is the angle of inclination of
 257 the rock unit measured from a horizontal plane, and (x_1, z_1) and (x_2, z_2) are the coordinates of the upper
 258 and lower boundaries of the rock unit (**Fig. 6**). Bott's simple criteria are as follows: when $|g''_{max}|$
 259 is greater than $|g''_{min}|$, then the anomaly can be attributed to a sedimentary basin with an inward sloping
 260 edge, whereas if $|g''_{max}|$ is smaller than $|g''_{min}|$, then the source of the anomaly is a granite pluton with
 261 an outward sloping edge. This study can be applied to fault analysis, especially in determining the
 262 direction of the fault's slope but not the fault type (Sumintadireja et al., 2018).

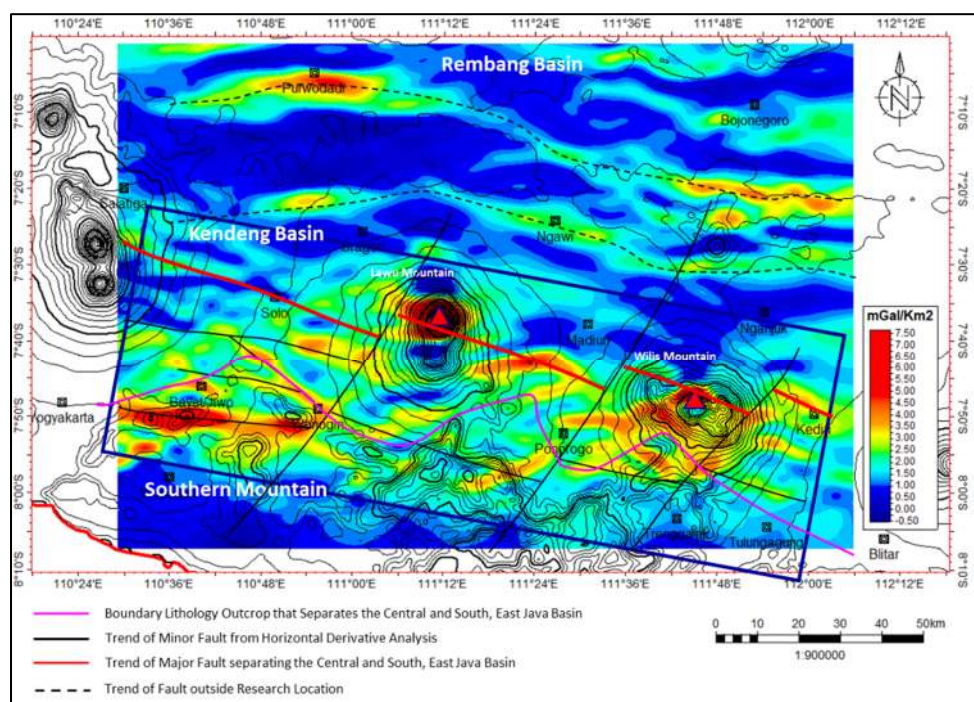
263



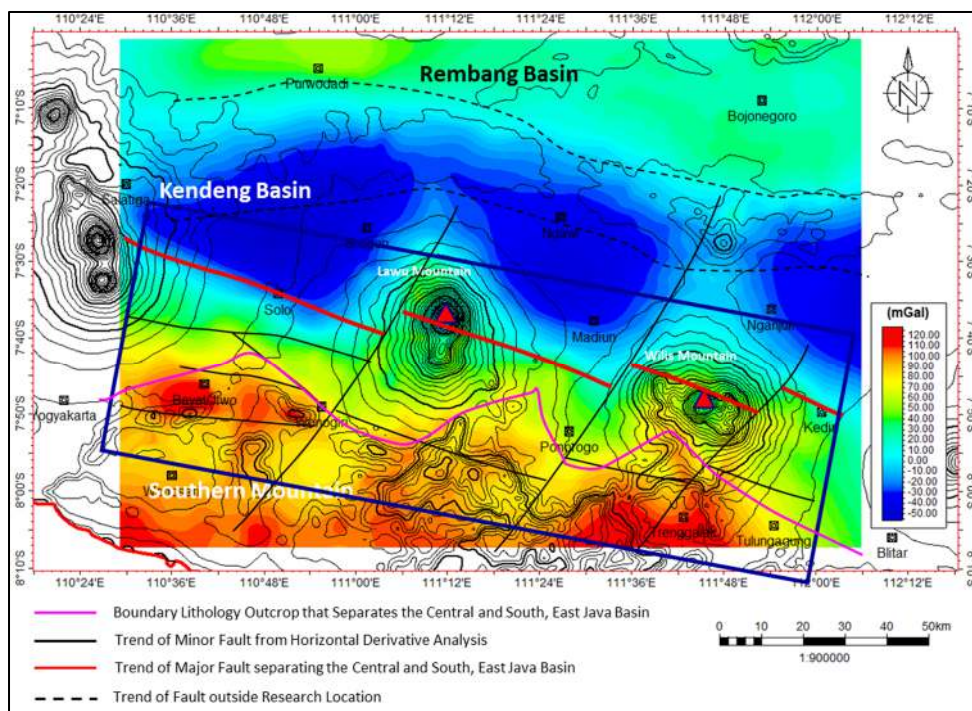
264
 265 **Fig. 6.** Gravity anomaly and SVD responses to the rock slope model wherein the SVD value (g'') reaches its
 266 maximum when ρ is negative (indicating a basin), decreases to the minimum value, then finally rises again
 267 asymptotically to zero (Bott, 1962).
 268
 269

270 **4. Results and Discussion**

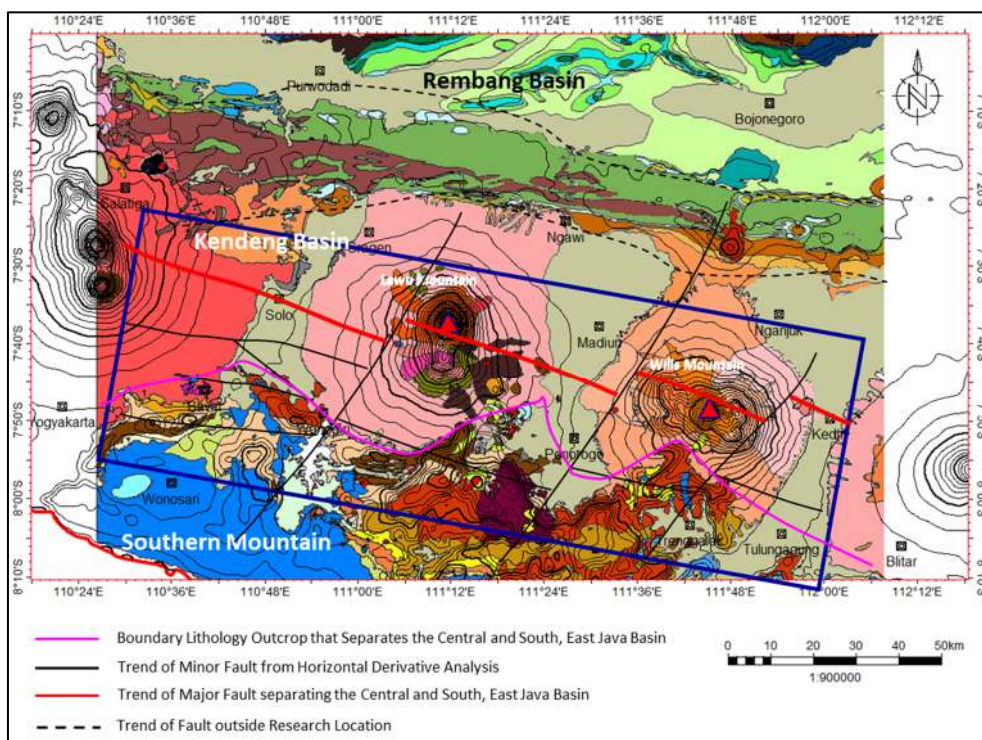
271 The subsurface boundary between the Southern Mountains and the Kendeng Basin was determined
 272 using the derivative method. Surface data identified that the two Quaternary volcanoes, Mount Wilis
 273 and Mount Lawu, produce volcanic deposits covering almost the entire interzonal boundary. Although
 274 surface identification of said boundary is not feasible, the west-east volcano lineage between Mount
 275 Lawu and Mount Wilis and several parallel volcanoes may indicate a weak zone through which magma
 276 emerges as a volcano. **Fig. 7** shows the results of the horizontal derivative analysis of the gravity data.
 277 Total Horizontal Derivative (THD) solidifies fine-sized features on the fault boundary plane, allowing
 278 the fault-associated boundary anomalies to produce strong derivative anomalies. Based on the horizontal
 279 derivative analysis, the boundary between the Southern Mountains and the basin in the north showed a
 280 strong lineage anomaly and is interpreted as a west-east trending major fault continuity (red line).
 281 Bouguer anomaly map, showed a contrasting pattern between the zones. The Southern Mountains were
 282 characterized by a high gravity anomaly between 130–50 mGal, while the Kendeng Basin had a much
 283 lower value of up to -50 mGal. This major fault limits the high Bouguer gravity anomaly area in the
 284 south with a low anomaly area in the north in subsurface conditions (**Fig. 8**). The major fault boundaries
 285 cannot be clearly identified on the surface because most of them are covered with Quaternary volcanic
 286 deposits. **Fig. 9** shows the subsurface fault interpretation plotted on the geological map. Some outcrops
 287 that are positionally out of Southern Mountain line indicate the presence of a major fault that displaced
 288 them from their zone, e.g., limestone outcrops of the Wonosari Formation on the western slope of Mount
 289 Lawu. This limestone is interpreted as moving northward from the Southern Mountains due to a thrust
 290 fault. Another indication is the presence of breccia outcrops of the Old Andesite Formation (OAF) group
 291 on the eastern side of Mount Lawu (Rachman, 2017). The outcrops are known to be the northernmost
 292 of the OAF outcrop group in the south, which is thought to have moved from its initial position due to
 293 a thrust fault.
 294



295 **Fig 7.** Horizontal derivative analysis results show the boundary structure line between the Kendeng Basin and the
 296 Southern Mountains. This structure extends in a relative west-east direction (The blue-line box marks the research
 297 location)
 298
 299
 300



301
 302 **Fig 8.** Fault interpretation from THD plotted on Bouguer Anomaly map. This major fault limits the high Bouguer
 303 gravity anomaly area in the south with a low anomaly area in the north (The blue-line box marks the research
 304 location)
 305



306
 307 **Fig 9.** The subsurface fault interpretation plotted on the geological map. (The blue-line box marks the research
 308 location)
 309

310 The SVD analysis was also applied to support the other derivative analyses. Both SVD and THD
 311 analyses confirm the anomaly identified in the fault boundary plane. The research created SVD cross-
 312 sections of two selected tracks to determine the slope pattern of the faults identified in the derivative

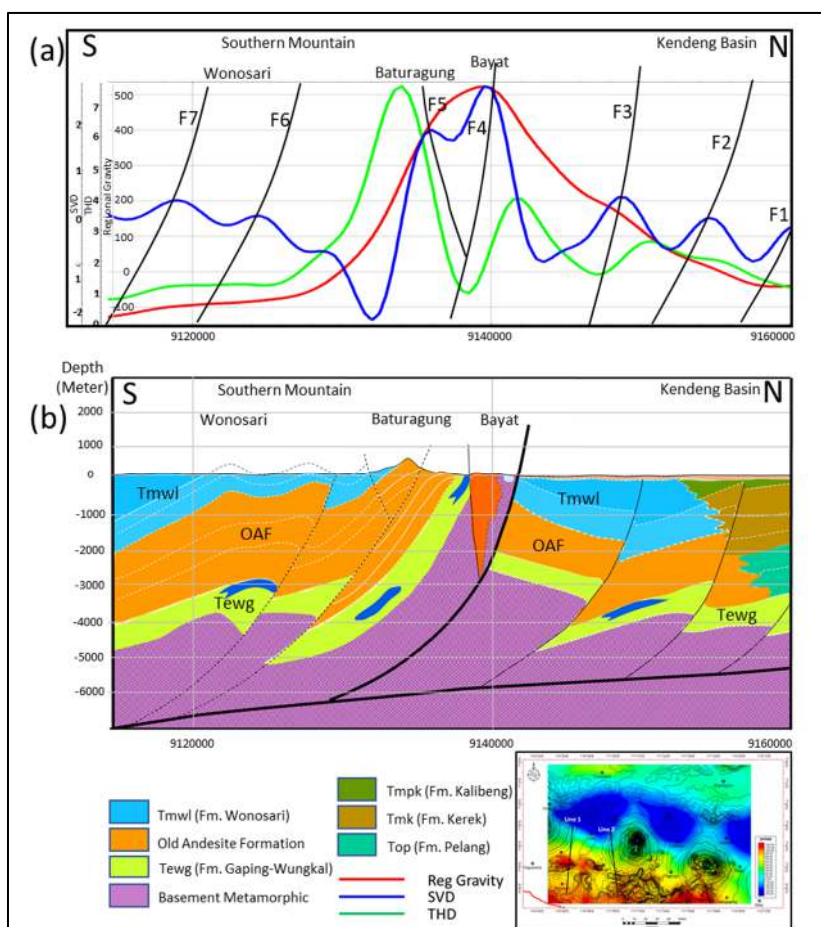
313 analysis. Combined with the density value, the absolute minimum and maximum SVD values show the
 314 slope gradients of the fault observed (**Tables 1 and 2**). Based on Bott's criteria, the fault slope is
 315 predominantly southward (**Fig. 10a and 11a**). This analysis result corresponds to the geological studies
 316 wherein the direction of stress induced by compressional tectonics from the Australia-Sundaland
 317 interaction is thought to form a thrust fault that tilts southward and a fold-thrust belt along the Southern
 318 Mountains and Kendeng Basin. The 2.5D gravity modeling produced the conceptual geological model
 319 of the fold-thrust belt formation, which shows a major fault with a south-facing slope that separates the
 320 two zones and forms the fold-thrust belt system with a steep slope in the south that slants down toward
 321 the south (Fig. 9b and 10b).

Table 1. SVD calculations for fault direction identification on Line 1

No	SVD min	SVD max	Density 1 (North)	Density 2 (South)	Dip Fault Orientation
F1	-0,9	-0,2	-39,8	-35,6	South
F2	-0,7	-0,09	13,2	64,5	South
F3	-0,9	0,4	162	341,1	South
F4	1,6	2,8	520,9	487,8	South
F5	-2,2	1,8	424,4	99,5	North
F6	-0,2	0,07	-81,5	-88,2	South
F7	-0,1	0,3	-96,6	-119,4	South

323

324



325

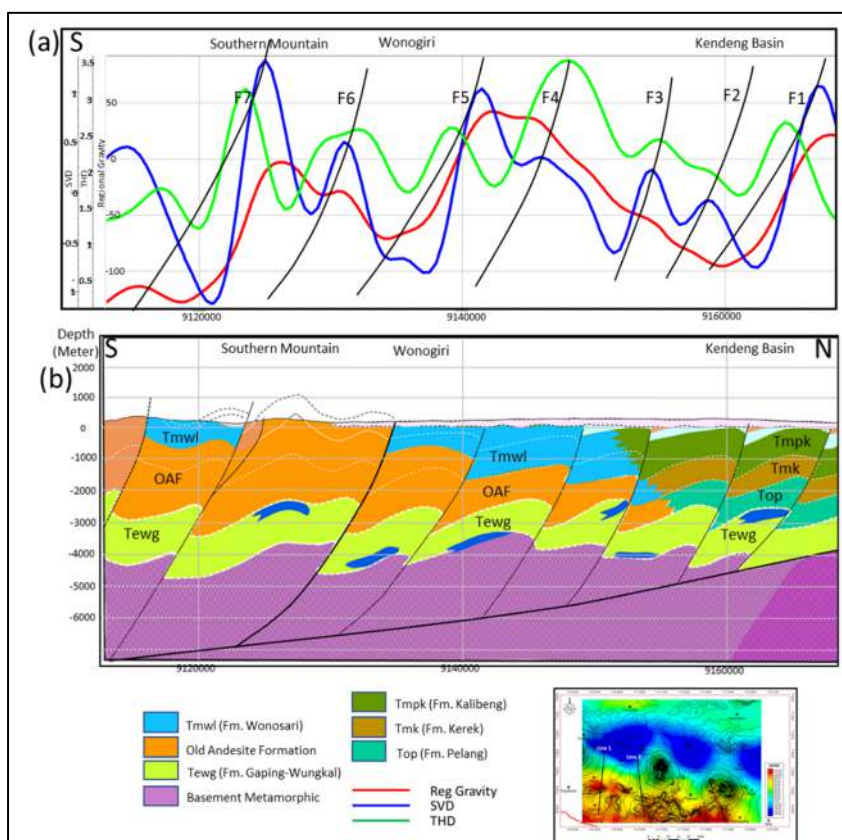
Fig 10. (a) A cross-section derived from the vertical derivative analysis results shows the fault slope direction on
 327 Line 1. (b) The geological model demonstrates the developing structural pattern in the Southern Mountains and
 328 Kendeng Basin.

329

Table 2. SVD calculations for fault direction identification on Line 2

No	SVD min	SVD max	Density 1 (North)	Density 2 (South)	Dip Fault Orientation
F1	-0,75	1,06	18,7	-77,7	South
F2	-0,32	-0,09	-92,6	-77,9	South
F3	-0,6	0,22	-55,3	-38,1	South
F4	0,28	0,35	37,2	32,9	South
F5	-0,8	1,04	38,9	-55,8	South
F6	-0,21	0,49	-30,8	-31,8	South
F7	-1,11	1,32	-11	-111,2	South

330
331
332



333
334
335
336

Fig. 11. (a) A cross-section derived from the vertical derivative analysis results shows the fault slope direction on Line 2. (b) The geological model demonstrates the developing structural pattern in the Southern Mountains and Kendeng Basin.

337 **5. Conclusions**

338 Eastern Java is formed by the compressive tectonics occurring in several periods in the Cenozoic
339 due to the interaction between the Gondwana microcontinent and southeastern Sundaland. The
340 compressive tectonics generate northward thrusting along southern Java and form the fold-thrust belt
341 system that expands northward to the Kendeng Basin. Indications of this tectonic activity have long
342 been identified, but the thick Quaternary volcanic deposits mask its precise boundaries.

343 Based on the total horizontal derivative analysis results, the anomaly shows a west-east continuity
344 interpreted as a fault continuity—the suspected boundary separating the Southern Mountains and the
345 Kendeng Basin in the north. Further, the second vertical derivative analysis results show that the major
346 fault interpreted as the interzonal boundary has a dominantly south-facing slope, which corresponds to
347 the stresses acting along the island of Java. The conceptual model made by 2.5D gravity data modeling

348 shows that the fault forms a fold-thrust belt system with the angle of the fault plane slanting down
349 northward. This thrust fault concept can explain how the rock constituents of the Southern Mountains
350 can move from the main path and shift further north.

351 **Acknowledgments:**

352 The authors are grateful to the Indonesian Geological Research and Development Center for publishing
353 accessible data for this research.

354 **References**

- 355 Bott, M.P.H., 1962. A Simple Criterion for Interpreting Negative Gravity Anomalies, *Geophysics*, 27(3), 376-381.
356 <https://doi.org/10.1190/1.1439026>
- 357 Hall, R., Clements, B., Smyth, H.R., Cottam, M.A., 2007. A New Interpretation Of Java's Structure, Proceedings
358 of Indonesian Petroleum Association Thirty-First Annual Convention and Exhibition, G-035.
359 https://doi.org/10.29118/ipa.1077.07.g.035_
- 360 Husein, S., Mustofa, A., Sudarno, I., Toha, B., 2008. Tegalrejo Thrust Fault As An Indication Of Compressive
361 Tectonics in Baturagung Range, Bayat, Central Java, 37th Annual Convention IAGI, 258-268.
362 DOI:[10.13140/RG.2.1.4234.3128](https://doi.org/10.13140/RG.2.1.4234.3128)
- 363 Lokier, S., 2000. The development of the Miocene Wonosari Formation, south Central Java, Indonesian,
364 Proceedings of Indonesian Petroleum Association 27th Annual Convention, pp. 217-222.
365 DOI:[10.29118/ipa.2049.g.027](https://doi.org/10.29118/ipa.2049.g.027)
- 366 Prasetyadi, C., Rachman, M.G., Hapsoro, S.E., Shirly, A., Gunawan, A., and Purwaman, I., 2016. Seismic-Based
367 Structural Mapping of RMKS Fault Zone: Implication to Hydrocarbon Accumulation in East Java Basin,
368 Proceedings Geosea XIV And 45th IAGI Annual Convention (GIC 2016), 104-107.
369 http://repo-nkm.batan.go.id/1088/1/PROSIDING_SUKADANA_PTBGN_2016.pdf
- 370 Rachman, M.G., 2017. Evolusi Tektonik Pegunungan Selatan Jawa Bagian Timur, thesis, Pembangunan Nasional
371 "Veteran" Yogyakarta University.
372 <http://eprints.upnyk.ac.id/id/eprint/13940>
- 373 Setiaji, R.A., Andhika C.A., Aulia, K.N., Radityo, D., Arifullah, E., 2016. The Stratigraphic Significance of
374 Glossifungites Ichnofacies in Cipari Area, Central Java, Proceedings Geosea XIV And 45th IAGI Annual
375 Convention (GIC 2016), 540-543.
376 http://repo-nkm.batan.go.id/1088/1/PROSIDING_SUKADANA_PTBGN_2016.pdf
- 377 Smyth, H.R., Hall, R., Hamilton, J., and Kinny, P., 2005. East Java: Cenozoic Basins, Volcanoes And Ancient
378 Basement, Proceedings of Indonesian Petroleum Association. Thirtieth Annual Convention & Exhibition,
379 251-266: G-045
380 <https://doi.org/10.29118/ipa.629.05.g.045>
- 381 Smyth, H.R., Hall, R., and Nichols, G.J., 2008. Cenozoic Volcanic Arc History Of East Java, Indonesia: The
382 Stratigraphic Record Of Eruptions On An Active Continental Margin, The Geological Society of America,
383 Special Paper 436, 199-222.
384 [https://doi.org/10.1130/2008.2436\(10\)](https://doi.org/10.1130/2008.2436(10))
- 385 Sumintadireja, P., Dahrin, D., and Grandis, H., 2018. A Note on the Use of the Second Vertical Derivative (SVD)
386 of Gravity Data with Reference to Indonesian Cases, *Journal Engineering Technol. Sci.*, Vol. 50 No. 1,
387 127-139.
388 <https://doi.org/10.5614/j.eng.technol.sci.2018.50.1.9>
- 389 Van Bemmelen, R.W., 1949. The Geology of Indonesia. Vol 1A. General Geology of Indonesia And Adjacent
390 Archipelagos, Martinus Nijhoff, The Hague, Netherlands.
- 391
- 392 Waltham, D., Hall, R., Smyth, H.R., and Ebinger, C.J., 2008. Basin formation by volcanic arc loading, The
393 Geological Society of America, Special Paper, 436, 11-26.
394 [https://doi.org/10.1130/2008.2436\(02\)](https://doi.org/10.1130/2008.2436(02))
- 395